

Differential involvement of endocytic compartments in the biosynthetic traffic of apical proteins

Kerry O Cresawn^{1,5}, Beth A Potter^{1,5},
Asli Oztan¹, Christopher J Guerriero¹,
Gudrun Ihrke³, James R Goldenring⁴,
Gerard Apodaca^{1,2} and Ora A Weisz^{1,2,*}

¹Renal-Electrolyte Division, University of Pittsburgh, Pittsburgh, PA, USA, ²Department of Cell Biology and Physiology, University of Pittsburgh, Pittsburgh, PA, USA, ³Department of Pharmacology, Uniformed Services University of the Health Sciences, Bethesda, MD, USA and ⁴Department of Surgery, Vanderbilt University School of Medicine and Nashville Veterans Affairs Medical Center, Nashville, TN, USA

Newly synthesized basolateral markers can traverse recycling endosomes en route to the surface of Madin–Darby canine kidney cells; however, the routes used by apical proteins are less clear. Here, we functionally inactivated subsets of endocytic compartments and examined the effect on surface delivery of the basolateral marker vesicular stomatitis virus glycoprotein (VSV-G), the raft-associated apical marker influenza hemagglutinin (HA), and the non-raft-associated protein endolyn. Inactivation of transferrin-positive endosomes after internalization of horseradish peroxidase (HRP)-containing conjugates inhibited VSV-G delivery, but did not disrupt apical delivery. In contrast, inhibition of protein export from apical recycling endosomes upon expression of dominant-negative constructs of myosin Vb or Sec15 selectively perturbed apical delivery of endolyn. Ablation of apical endocytic components accessible to HRP-conjugated wheat germ agglutinin (WGA) disrupted delivery of HA but not endolyn. However, delivery of glycosylphosphatidylinositol-anchored endolyn was inhibited by >50% under these conditions, suggesting that the biosynthetic itinerary of a protein is dependent on its targeting mechanism. Our studies demonstrate that apical and basolateral proteins traverse distinct endocytic intermediates en route to the cell surface, and that multiple routes exist for delivery of newly synthesized apical proteins.

The EMBO Journal (2007) 26, 3737–3748. doi:10.1038/sj.emboj.7601813; Published online 2 August 2007

Subject Categories: membranes & transport

Keywords: biosynthetic delivery; endosome; lipid raft; MDCK; polarized

Introduction

The generation and maintenance of the apical and basolateral surfaces in polarized epithelial cells requires efficient sorting and proper trafficking of proteins along the biosynthetic and postendocytic pathways. Protein sorting mechanisms rely on the recognition of sorting signals inherent within proteins. Basolateral sorting signals generally comprise linear peptide sequences within the cytoplasmically disposed regions of proteins, some of which fit consensus binding motifs for recognition by adaptor protein complexes (Rodriguez-Boulau *et al*, 2005). In contrast, apical sorting has been shown to depend on a wide variety of signals, including cytoplasmic peptide motifs, protein association with glycolipid-enriched, detergent-resistant microdomains (herein referred to as lipid rafts) through lipid anchors or transmembrane residues, and both N- and O-glycans (Rodriguez-Boulau *et al*, 2005; Ellis *et al*, 2006). Recognition of these sorting signals is thought to occur in the *trans*-Golgi network (TGN) based on morphological and biochemical studies demonstrating the segregation of TGN-staged apical and basolateral cargo into discrete vesicles (Wandinger-Ness *et al*, 1990; Keller *et al*, 2001; Kreitzer *et al*, 2003). Although the conventional model for biosynthetic protein sorting posited that post-Golgi vesicles are delivered directly to the plasma membrane, several studies over the past several years have suggested instead that some cargo traffics to the surface via endocytic intermediates (Futter *et al*, 1995; Leitinger *et al*, 1995; Orzech *et al*, 2000; Ang *et al*, 2004).

Several proteins have been shown to traffic to the surface via endocytic compartments in nonpolarized cells. Results from density shift assays and endosome immunoprecipitation experiments, respectively, suggest that newly synthesized transferrin (Tf) receptor (Futter *et al*, 1995) and the asialoglycoprotein receptor (Leitinger *et al*, 1995) transit endocytic compartments prior to surface delivery. More recently, a temperature-sensitive mutant of the vesicular stomatitis virus glycoprotein (VSV-G) conjugated to yellow fluorescent protein (tsVSV-G-YFP) was shown by Ang *et al* (2004) to transit Tf-positive recycling endosomes before delivery to the surface. The indirect trafficking of tsVSV-G-YFP appears necessary for proper delivery, as inactivation of Tf-positive recycling endosomes inhibited subsequent delivery of tsVSV-G-YFP to the surface (Ang *et al*, 2004). Similarly, Lock and Stow (2005) used live cell imaging techniques to demonstrate trafficking of pre-staged E-cadherin from the TGN to Rab11-positive recycling endosomes of HeLa cells.

Endocytic recycling compartments have also been implicated in biosynthetic trafficking in polarized cells; however, the organization of endocytic compartments is more complex in these cells. There are distinct populations of apical and basolateral early endosomes, a common recycling endosome (CRE) accessible to both apically and basolaterally internalized cargo, and a Rab11-positive apical recycling endosome

*Corresponding author. Renal-Electrolyte Division, University of Pittsburgh, 3550 Terrace St., Pittsburgh, PA 15261, USA.
Tel.: +1 412 383 8891; Fax: +1 412 383 8956;
E-mail: weisz@pitt.edu

⁵These authors equally contributed to this work

Received: 12 January 2007; accepted: 4 July 2007; published online: 2 August 2007

(ARE). The CRE plays an important role in segregating apical and basolateral cargo, whereas the ARE is primarily involved in regulation of apically directed traffic (Hoekstra *et al*, 2004). The ARE has been shown to be physically and functionally distinct from other apical endocytic compartments and is typically characterized by the presence of rab11a and immunoglobulin A (IgA) and the absence of Tf (Apodaca *et al*, 1994; Barroso and Sztul, 1994; Gibson *et al*, 1998; Brown *et al*, 2000). A significant fraction of newly synthesized, basolaterally destined polymeric immunoglobulin receptor (pIgR) was shown to traverse the Tf-positive CRE before surface delivery (Orzech *et al*, 2000), suggesting that basolateral proteins transit recycling endosomes in polarized as well as nonpolarized cells. However, it remains unclear whether apical proteins also traverse endocytic compartments along the biosynthetic pathway. In previous studies, missorted apically targeted mutants of VSV-G and pIgR were suggested to transit endocytic compartments en route to the cell surface; however, the 'apical' variants used in these experiments possess basolateral sorting motifs that could be recognized by basolateral sorting machinery (Orzech *et al*, 2000; Ang *et al*, 2004). Additionally, there is evidence that apical proteins with different targeting signals are delivered to the surface in distinct populations of transport carriers (Jacob and Naim, 2001; Polishchuk *et al*, 2004); thus, there may be multiple biosynthetic routes to the apical surface. Consistent with this idea, several studies have demonstrated selective involvement of actin-dependent trafficking mechanisms in the transport of lipid-raft associated apical proteins (Jacob *et al*, 2003; Heine *et al*, 2005; Guerriero *et al*, 2006).

To address the involvement of endocytic compartments in apical trafficking, we have selectively perturbed the function of subsets of endocytic compartments and examined the consequences on surface delivery of two proteins: the non-raft-associated protein endolyn and raft-associated hemagglutinin (HA). Endolyn is a sialomucin that efficiently traffics to the apical surface from the TGN of polarized Madin–Darby canine kidney (MDCK) cells, and subsequently cycles constitutively between the surface and lysosomes (Ihrke *et al*, 2001, 2004; Potter *et al*, 2006). Our previous studies have revealed that biosynthetic and postendocytic apical delivery of endolyn is dependent on the terminal processing of a subset of N-glycans within its luminal domain (Potter *et al*, 2004, 2006). In contrast, apical delivery of HA is dependent on sorting information contained within the single transmembrane domain of this protein (Lin *et al*, 1998). Our results suggest that newly synthesized apical and basolateral proteins access different populations of endosomes after leaving the TGN, and moreover, that raft-associated and raft-independent proteins take different routes via distinct endocytic intermediates to the apical surface.

Results

Apically destined proteins do not traverse the CRE en route to the cell surface

As described above, recent studies using a temperature-sensitive variant of VSV-G have demonstrated that this protein enters Tf-positive recycling endosomes before surface delivery in MDCK cells (Ang *et al*, 2004). This study relied on immunofluorescence, electron microscopy, and immunoisolation approaches made possible by the ability to accumulate

significant levels of tsVSV-G-YFP in the endoplasmic reticulum by incubation at the nonpermissive temperature, 40°C. In compelling experiments, Tf conjugated to horseradish peroxidase (HRP) was internalized into recycling endosomes and the cells were then treated with diaminobenzidine (DAB) and hydrogen peroxide to form an insoluble precipitate that prevented fusion of post-Golgi vesicles with this compartment and consequently inhibited surface delivery of tsVSV-G-YFP. Because analogous temperature-sensitive variants are not available for most apical markers, we first confirmed the immunofluorescence results of Ang *et al* (2004) using subconfluent MDCK cells, and then developed a biochemical approach that would enable us to quantitate the effects of endosome ablation on surface delivery of radiolabeled apical and basolaterally directed biosynthetic cargo in fully polarized MDCK cells.

MDCK cells that stably express human Tf receptor (TfR; PTR9 cells) were grown on coverslips and infected with replication-deficient adenovirus encoding tsVSV-G-YFP and incubated at 40°C overnight to accumulate the protein in the endoplasmic reticulum. The next day, HRP-Tf was internalized basolaterally for 45 min at 40°C to allow accumulation in recycling endosomes. To inactivate recycling endosomes, cells were incubated with DAB and 0.025% hydrogen peroxide for 1 h on ice. As additional controls, we omitted either the HRP-Tf incubation (no HRP-Tf) or the hydrogen peroxide (no H₂O₂) in these experiments. After a 1-h chase at the permissive temperature of 32°C in the presence of cycloheximide to prevent new protein synthesis, the cells were fixed and imaged (Figure 1A). In concordance with the observations of Ang *et al* (2004), delivery of tsVSV-G-YFP to the surface was only inhibited when recycling endosomes were successfully inactivated by incubation with both DAB and hydrogen peroxide.

We next modified this protocol to enable quantitation of the effects of inactivating Tf-positive CRE on basolateral delivery of radiolabeled VSV-G in fully polarized cells. These and our other biochemical experiments were variously performed using adenoviruses encoding either tsVSV-G-YFP or wild-type VSV-G; and because we obtained indistinguishable results with both, the data have been combined. In the description of these experiments, the term VSV-G thus refers to both constructs. Virally-infected filter-grown PTR9 cells were radiolabeled for 15 min in the presence or absence of HRP-Tf and the cells were incubated with or without DAB and hydrogen peroxide for 1 h on ice. Cells were then chased at 37°C (for VSV-G) or 32°C (for tsVSV-G-YFP) for 0 or 90 min, after which the basolateral surface was biotinylated. A representative gel from one experiment is shown in Figure 1B. Consistent with our immunofluorescence results in Figure 1A, quantitation of the results from several biochemical experiments confirmed that inactivation of HRP-Tf containing endosomes significantly inhibited basolateral delivery of VSV-G by about 50%. VSV-G was not missorted to the apical surface under these conditions, as CRE inactivation had no effect on the total amount of VSV-G delivered to the apical plasma membrane (KO Cresawn and BA Potter, unpublished data, 2007).

Having validated our biochemical approach to examine the itinerary of VSV-G, we next determined the effect of inactivating the CRE on apical trafficking of endolyn and HA. These experiments were performed essentially as described for

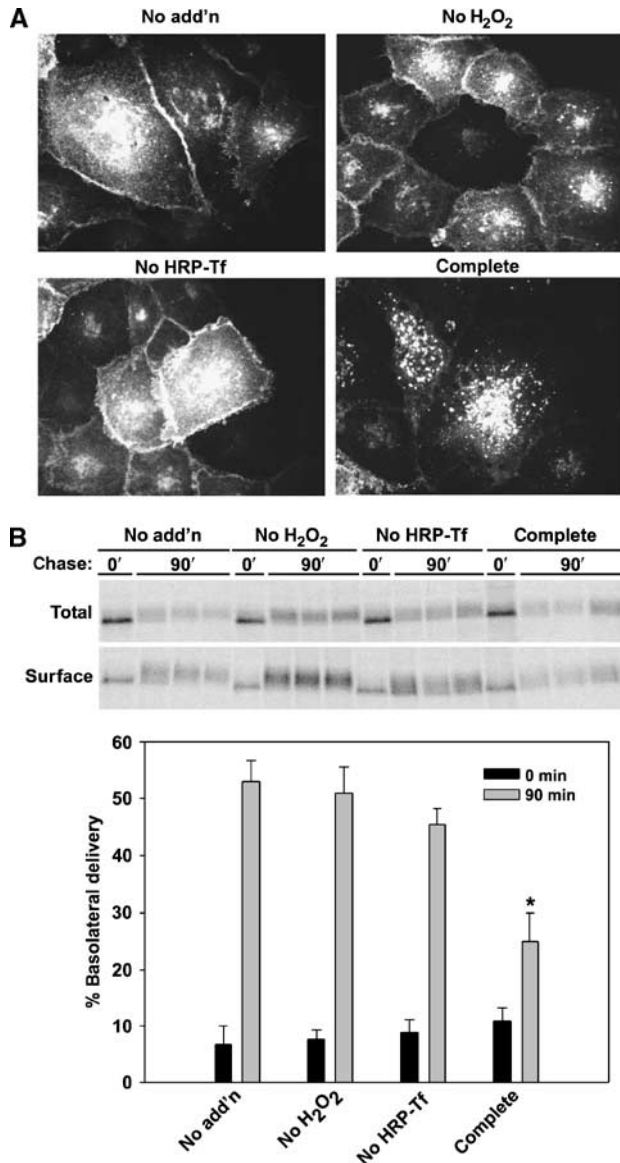


Figure 1 Inactivation of Tf-containing endosomes in nonpolarized and polarized cells inhibits surface delivery of tsVSV-G-YFP. (A) PTR9 cells grown on coverslips were infected with adenovirus-encoding tsVSV-G-YFP and incubated overnight at 40°C. The next day, the cells were incubated in serum-free media for 30 min before addition of HRP-Tf for 45 min at 40°C. Remaining surface HRP-Tf was stripped and Tf-containing endosomes were inactivated on ice as described in Materials and methods. As controls in this and subsequent experiments, cells were incubated either without HRP-Tf, DAB, or H₂O₂ (no add'n), with only HRP-Tf and DAB (no H₂O₂), or with only DAB and H₂O₂ (no HRP-Tf). Cells were then incubated at 32°C in the presence of cycloheximide for 1 h, washed with PBS, then fixed and imaged. Scale bar = 5 μm (B) Polarized PTR9 cells grown on filters were infected with adenovirus encoding VSV-G and incubated overnight at 37°C. The following day, cells were starved in medium devoid of cysteine and methionine for 30 min and then radiolabeled for 15 min. HRP-Tf was included in the basolateral medium during the starve and radiolabeling period. After stripping residual surface HRP-Tf, cells were treated with or without DAB and H₂O₂ for 1 h on ice as in (A). After washing, cells were chased for 0 or 90 min at 37°C, and delivery to the basolateral surface was quantified using domain-selective biotinylation. Samples were immunoprecipitated and analyzed by SDS-PAGE and gels showing the total amount of radiolabeled protein in the cell and the amount at the basolateral surface in a representative experiment are shown (upper panel). The mean ± s.e. of three experiments is plotted (lower panel). Surface delivery of VSV-G was significantly inhibited in the 'complete' reaction samples compared with all three control conditions (**P* < 0.02 by Student's *t*-test).

Figure 1B, except that apical delivery of radiolabeled HA was quantitated using a cell surface trypsinization assay. Strikingly, inactivation of the CRE did not significantly decrease the amount of newly synthesized endolyn (Figure 2A) or HA (Figure 2B) that reached the apical surface, suggesting that these proteins do not traverse the CRE along the biosynthetic pathway. In these experiments, we routinely observed that a population of immature (nonsialylated) protein was recovered in the biotinylated fraction of all samples treated with hydrogen peroxide, suggesting that terminal glycosylation is perturbed by this reagent (compare surface 90 min *no HRP-Tf/complete* lanes with *no add'n* lanes). This was also the case for VSV-G (Figure 1B); however, the electrophoretic mobility shift is less obvious as this protein has only two N-linked glycans. Regardless, the aberrant glycosylation did not apparently perturb the efficiency of surface delivery, as surface delivery of fully and aberrantly processed endolyn was similar when the two fractions were quantitated separately (data not shown). This was somewhat surprising as we have previously shown that terminal glycosylation of endolyn N-glycans is required for polarized apical delivery (Potter *et al*, 2004). We hypothesize that peroxide may not affect the key determinant required for apical targeting, or alternatively, because only a fraction of endolyn is affected, multimerization or other mechanisms may compensate to enable efficient delivery of the entire pool of newly synthesized proteins.

Apical protein delivery is differentially sensitive to perturbation of ARE function

Given the segregation of recycling compartments in polarized cells, we next asked whether endolyn and HA traverse the ARE along the biosynthetic pathway. Attempts to generate a functional HRP-IgA conjugate to inactivate this compartment were unsuccessful. As an alternative, we examined the apical trafficking of endolyn and HA in MDCK cells stably expressing an inducible GFP-tagged myosin Vb tail fragment (GFP-MyoVbT) which acts as a dominant-negative inhibitor of membrane traffic out of the ARE (MyoVbT cells; Lapierre *et al*, 2001). This construct can interact with Rab11, but lacks a motor domain, and has previously been shown to cause the accumulation of transcytosing and apical recycling cargo in the ARE (Lapierre *et al*, 2001). To confirm this phenotype, we examined by immunofluorescence microscopy whether IgA internalized from the basolateral surface for 10 min and chased for 1 h accumulates in a GFP-positive subapical compartment as previously reported (Lapierre *et al*, 2001). Confocal images of optical sections through the subapical region reveal an accumulation of IgA in the ARE of MyoVbT cells not seen in parental MDCK cells (Figure 3A, panels b and d, respectively). Additionally, basolateral to apical transcytosis of pre-internalized ¹²⁵IgA was reduced by 35% after 1 h in MyoVbT cells compared with control cells, consistent with a perturbation of trafficking from the ARE in these cells (CJG, unpublished data, 2006).

To examine the effect of perturbing ARE function on the apical delivery of endolyn and HA, MyoVbT or control cells were infected with recombinant adenovirus expressing either construct. Cells were radiolabeled for 15 min and subsequent delivery of endolyn or HA to the apical surface was assessed upon warming the cells for 0, 30, 60, or 90 min at 37°C. As shown in Figure 3B, apical delivery of endolyn was significantly inhibited in MyoVbT cells compared to controls.

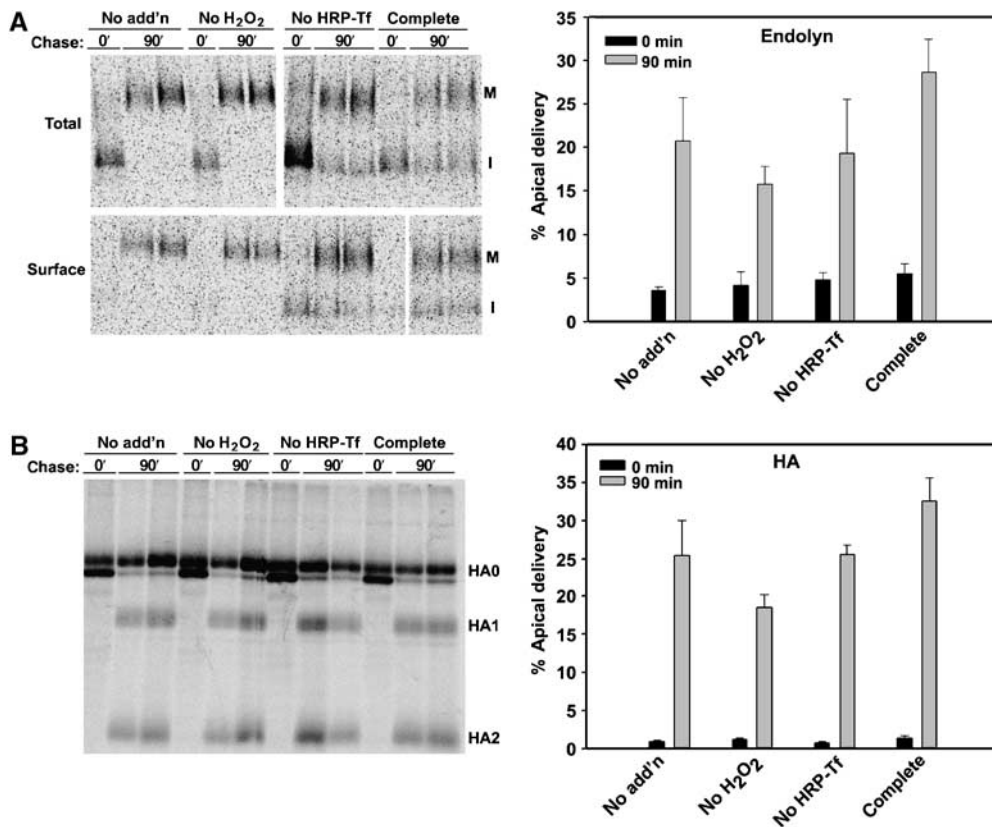


Figure 2 Delivery of endolyn and HA to the apical surface is not disrupted when Tf-containing endosomes are inactivated. Filter-grown PTR9 cells were infected with adenoviruses encoding endolyn (A) or HA (B) and incubated overnight at 37°C. Cells were radiolabeled, incubated with HRP-Tf at 37°C, and subjected to crosslinking as described for Figure 1B. Apical delivery was quantified by domain-selective biotinylation for endolyn (M = mature, I = immature) and by cell surface trypsinization for HA (resulting in two cleaved products marked HA1 and HA2). Uncleaved (intracellular) HA is marked as HA0. Samples were analyzed by SDS-PAGE and the gels from a representative experiment for each marker are shown (left panels). The percent apical delivery (mean ± s.e.m.) for endolyn ($n = 3$) and HA ($n = 3-6$) are shown (right panels). Surface delivery of HA and endolyn in the 'complete' reaction samples was statistically indistinguishable from all three control conditions.

Inhibition was observed even at the earliest time point, suggesting that biosynthetic rather than postendocytic delivery of endolyn was disrupted. In contrast, apical delivery kinetics of HA were comparable in both parental and MyoVbT cell lines (Figure 3C). Similarly, there was no effect on the kinetics of basolateral delivery of VSV-G in MyoVbT cells (Figure 3D), suggesting that of these three cargoes, only endolyn traverses the ARE en route to the surface.

As a complementary approach, we examined the effect of another perturbant of Rab11 function on apical delivery kinetics of endolyn and HA. Two hybrid analysis using *Drosophila* and canine homologs have revealed an interaction between Rab11a and the C-terminal domain of the Sec15 subunit of the exocyst (Zhang *et al*, 2004; Wu *et al*, 2005) and recent studies in MDCK cells have implicated a functional role for this interaction in IgA transcytosis (Oztan *et al*, in press). In these studies, expression of a C-terminal construct of Sec15 fused to GFP (Sec15CT) in polarized MDCK cells resulted in the redistribution of Rab11a and slowed transcytosis kinetics, but did not alter apical recycling of IgA. In contrast, expression of a GFP-tagged Sec15CT construct containing a point mutation that disrupts the interaction of the protein with Rab11 [Sec15CT(NA), in which Asn₇₀₉ is replaced by alanine] did not inhibit transcytosis (Oztan *et al*, in press). For our experiments, MDCK cell lines stably expressing

Sec15CT or Sec15CT(NA) were infected with adenovirus-expressing endolyn or HA and apical delivery of the proteins was quantitated as described above. Apical transport kinetics of endolyn were inhibited in cells expressing Sec15CT compared with parental cells and cells stably expressing the Sec15CT(NA) mutant (Figure 4A). In contrast, HA delivery was unaffected by expression of either Sec15CT construct (Figure 4B).

We used indirect immunofluorescence microscopy as a third approach to examine whether newly synthesized endolyn traverses a MyoVbT-/Rab11a-positive compartment en route to the apical surface. Endolyn was briefly expressed in MyoVbT cells via adenovirus and then incubated at 19°C for 2 h to accumulate newly synthesized biosynthetic cargo in the TGN. Cells were then warmed to 37°C for 20 min, fixed, incubated with antibodies to detect endolyn and Rab11a, and processed for confocal microscopy (Figure 5). Before warm-up, endolyn and rab11a were localized to distinct nonoverlapping compartments (data not shown). However, after warming for 20 min, significant colocalization between endolyn, GFP-MyoVbT, and Rab11a was observed (Figure 5C, E, and F). In contrast, no colocalization between HA staged in a similar fashion and GFP-MyoVbT was observed (Supplementary Figure 1). To ensure that the colocalization between endolyn and MyoVbT did not reflect postendocytic trafficking of endolyn that had reached the apical surface,

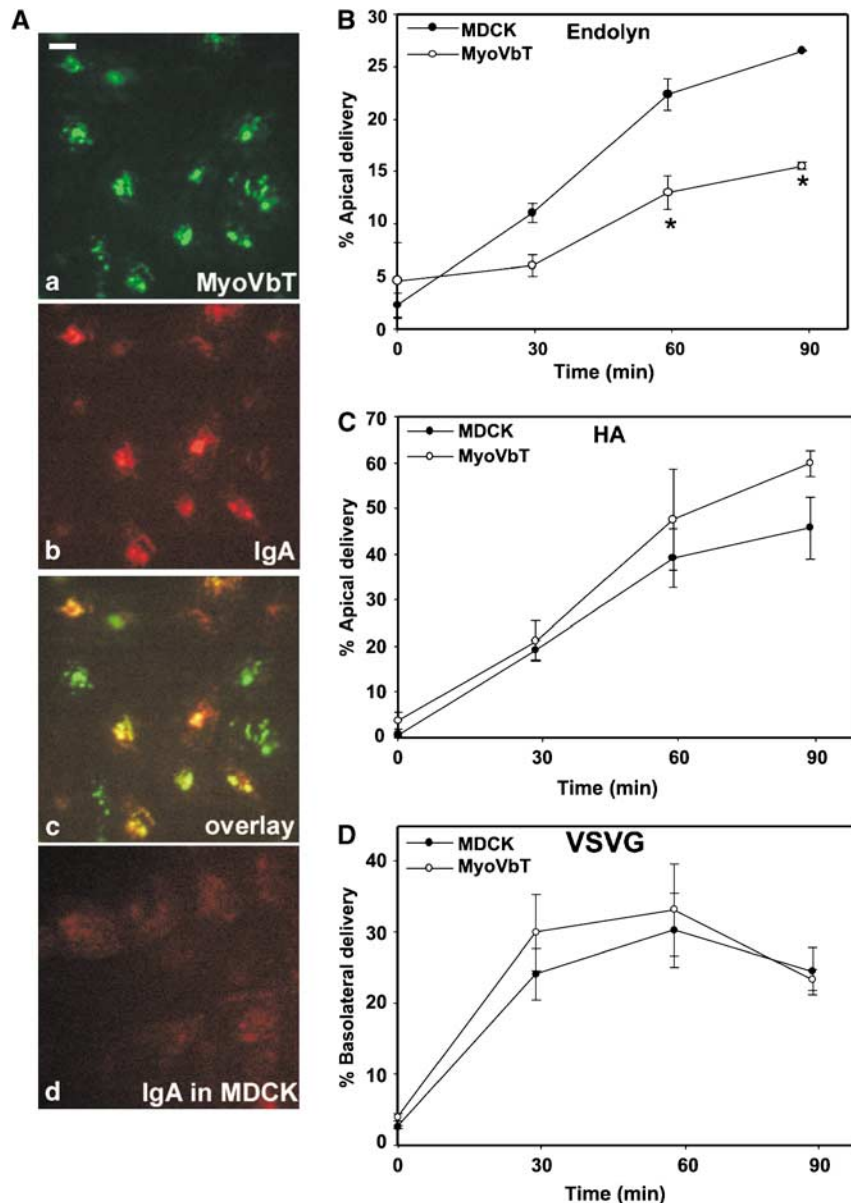


Figure 3 Biosynthetic apical delivery of endolyn, but not HA, is disrupted in cells expressing the myosin Vb tail. (A) IgA (200 µg/ml) was internalized from the basolateral surface of filter-grown MyoVbT or control MDCK cells for 10 min and chased for 60 min at 37°C. After rinsing, the cells were fixed, permeabilized, and incubated with Cy-5-conjugated anti-human IgA. Confocal sections taken just beneath the apical pole of the cell are shown; panel a: GFP-MyoVbT; panel b: IgA; panel c: overlay of a and b; panel d: IgA in control MDCK cells. Scale bar = 10 µm. (B–D) Filter-grown MyoVbT or control cells were infected with adenoviruses encoding endolyn (B), HA (C), or VSV-G (D). The following day, cells were starved, radiolabeled for 15 min, and chased for the indicated periods at 37°C before quantitation of surface delivery. The percent surface delivery is plotted as the mean ± range of two experiments with duplicate samples for endolyn and HA and four experiments for VSV-G. **P* < 0.001 compared with control cells.

some filters were incubated with anti-endolyn antibody during the last hour of the 19°C stage, then washed and incubated at 37°C for 20 min to track the route of any endolyn already at the surface before warming (Figure 5H). Internalized anti-endolyn antibody did not colocalize with GFP-MyoVbT, suggesting that endolyn recycles primarily from other apical endocytic compartments. Colocalization between post-TGN endolyn and rab11a was also observed in parental cells (Supplementary Figure 2). Together with the results from the MyoVbT and Sec15CT cell experiments, these data suggest that there are differential requirements for endocytic compartments in the delivery of subsets of apical proteins along the biosynthetic pathway, and point to a

selective involvement of the ARE in apical biosynthetic trafficking of endolyn but not HA.

Inactivation of HRP-wheat germ agglutinin-containing compartments selectively disrupts apical delivery of HA

Although the studies above suggest a role for the ARE in apical delivery of endolyn, they do not rule out the possibility that newly synthesized apical proteins traverse other apical endocytic compartments before cell surface delivery. We therefore examined whether internalization of wheat germ agglutinin (WGA) would provide access to a broader subset of apical endocytic compartments. WGA binds GlcNAc- or sialic acid-containing oligosaccharides on glycosylated

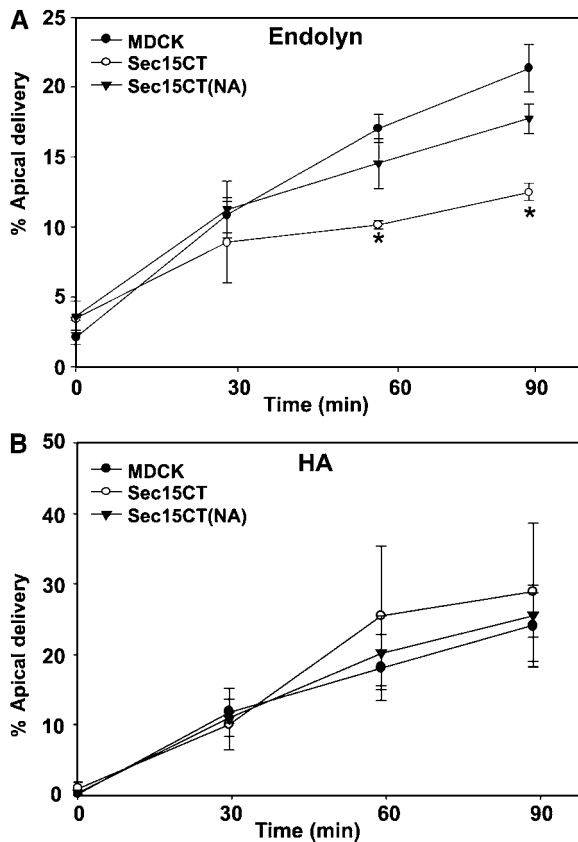


Figure 4 Expression of a dominant-negative inhibitor of Sec15 selectively disrupts apical delivery of endolyn. MDCK cells stably expressing Sec15 or Sec15(NA) and parental cells were co-infected with adenovirus-expressing transactivator and either endolyn (A) or HA (B). The following day, cells were radiolabeled for 15 min and chased from 0 to 90 min at 37°C before quantitation of apical delivery. The percent surface delivery is plotted as the mean \pm s.e. of three experiments for endolyn and two for HA. * $P < 0.05$ compared with control cells.

membrane proteins and is efficiently internalized into the apical endocytic pathway. To characterize which compartments WGA can access when internalized from the apical surface of polarized MDCK cells, FITC-conjugated WGA was internalized apically for 15 min at 37°C. Cells were then fixed, permeabilized, and processed with antibodies for markers of various compartments: the ARE marker Rab11a; the early endosome marker EEA1; the TGN marker furin; the late endosome marker mannose-6-phosphate receptor; and the lysosomal marker Lamp2. There was extensive colocalization of internalized FITC-WGA with the early endosomal marker EEA1 (Figure 6B). We also noted some overlap with the cation-independent mannose-6-phosphate receptor and, to a limited extent, with Lamp2 (Figure 6D and E). FITC-WGA did not colocalize with furin (Figure 6C). Surprisingly, we observed no colocalization between FITC-WGA and either Rab11a (Figure 6A) or Rab11b (KO Cresawn, unpublished data, 2001). Similar patterns of colocalization were also observed when FITC-WGA was internalized for 1 h at 19°C. Thus, WGA appears to efficiently access apical early endosomal compartments, but is selectively excluded from the ARE.

To examine the effect of ablating these compartments on biosynthetic membrane traffic biochemically, we internalized HRP-WGA from the apical surface for either 15 min at 37°C

(during the radiolabeling period) or subsequently for 1 h at 19°C before incubation with hydrogen peroxide and DAB on ice. We then quantitated cell surface delivery upon warm-up to 37°C for 0 or 90 min. We obtained indistinguishable results using either internalization condition, so the data were combined to generate the graphs shown in Figure 7. In contrast to the inhibitory effect of disrupting Rab11 function on apical delivery of endolyn, inactivation of HRP-WGA-containing compartments had no effect on apical delivery of this protein (Figure 7A). Delivery of p75, another detergent soluble apical transmembrane protein whose targeting signal has been localized to a heavily O-glycosylated domain (Yeaman *et al*, 1997), was also unaffected (KO Cresawn and BA Potter, unpublished data, 2006). Apical delivery of HA, however, was inhibited (Figure 7B; $16.2 \pm 0.9\%$ in the 'complete' reaction versus $31.6 \pm 4.7\%$ in the 'no add'n' control). We also evaluated the effect of apical HRP-WGA internalization on basolateral delivery of VSV-G, and found no effect (Figure 7C). These results suggest that non-raft-associated and raft-associated cargoes access distinct endocytic compartments en route to the apical surface.

Conversion of endolyn to a glycosylphosphatidylinositol-anchored protein renders its apical delivery sensitive to inhibition by HRP-WGA

To confirm that inactivation of HRP-WGA-containing compartments selectively disrupts delivery of raft-associated cargo, we examined the trafficking of a glycosylphosphatidylinositol (GPI)-anchored version of endolyn. Previous studies have shown that this protein is delivered to the apical surface in a glycan-independent manner and is partly insoluble in cold Triton X-100 (similar to HA), suggesting that it is delivered by a raft-associated mechanism (Potter *et al*, 2004). Consistent with our hypothesis, inactivation of HRP-WGA-containing compartments inhibited delivery of GPI-endolyn to the apical surface by $>50\%$ (Figure 8; $14.9 \pm 1.2\%$ in the 'complete' reaction versus $31.2 \pm 5.1\%$ in the 'no add'n' control). Decreased surface expression of GPI-endolyn was even more profound at an early (15 min) chase time ($2.6 \pm 0.1\%$ at the apical surface for 'complete' reaction after 15 min chase versus $17.8 \pm 1.8\%$ for 'no add'n' control; $n = 2$ experiments performed in duplicate, data not shown) suggesting that the effect was not due to inhibition of GPI-endolyn recycling. Conversely, inactivation of HRP-WGA-containing compartments failed to inhibit apical delivery of a raft-independent mutant of HA (A517; (Lin *et al*, 1998)) compared with controls (Supplementary Figure 3). Thus, the trafficking itinerary of a given protein can be rerouted by altering its apical targeting mechanism.

Discussion

Recent studies by several laboratories have suggested that the complexity of biosynthetic sorting in polarized epithelial cells is greater than initially envisioned. Here, we have attempted to define the post-Golgi routes taken by newly synthesized apically destined proteins. We find that the surface delivery of newly synthesized apical proteins is differentially affected upon perturbation of endocytic function. Our results support the idea that apical markers whose sorting is mediated by different mechanisms are largely segregated into distinct post-Golgi carriers. Moreover, these carriers access

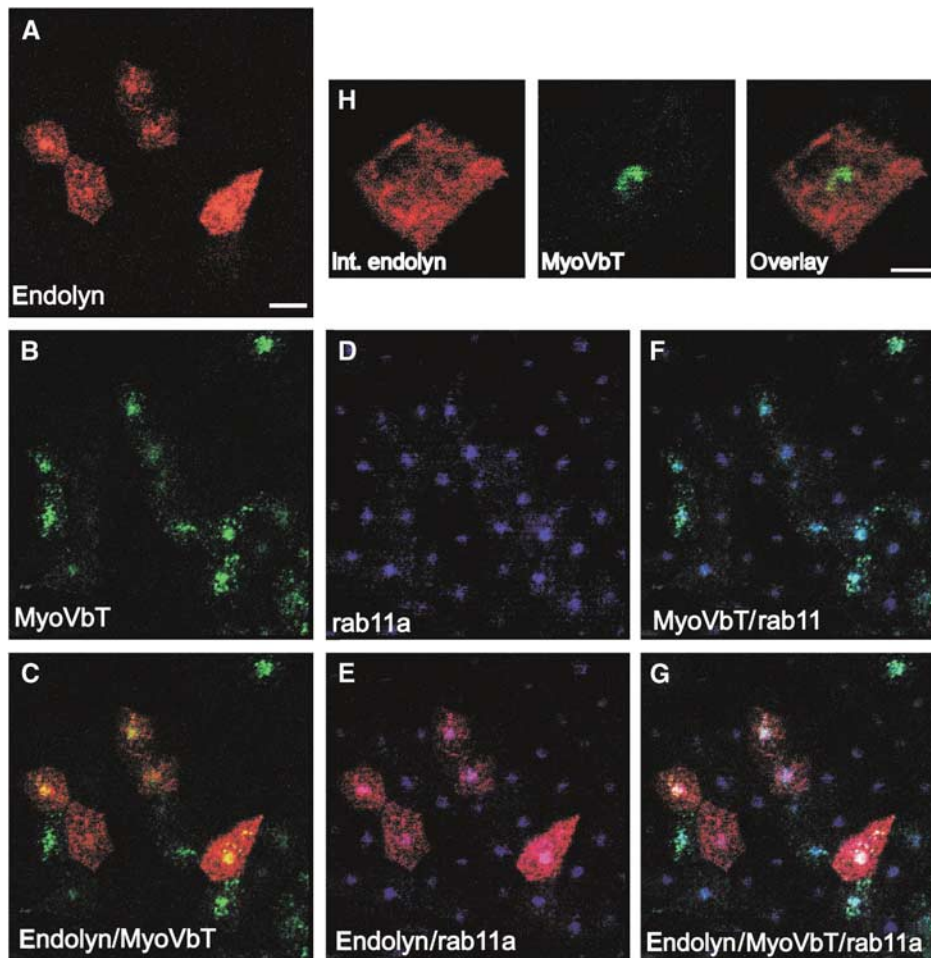


Figure 5 Newly synthesized endolyn colocalizes with MyoVbT and rab11a. Filter-grown MyoVbT cells were infected with adenovirus-expressing endolyn, incubated for 6 h at 37°C to initiate endolyn synthesis, and then moved to 19°C for 2 h to accumulate newly synthesized proteins in the TGN. Cells were then warmed to 37°C for 20 min to release staged proteins, then fixed and processed for detection of GFP-MyoVbT (green (B)), endolyn (red (A)), and rab11a (blue (D)). Individual confocal sections taken just beneath the apical pole of the cell are shown in each panel. Colocalization of GFP-MyoVbT with rab 11a is shown in (F); overlay of endolyn with GFP-MyoVbT, rab11a, and the triple overlay are shown in (C), (E), and (G), respectively. Cells in (H) were incubated with apically added monoclonal anti-endolyn antibody during the last hour at 19°C, then warmed to 37°C for 20 min to track the postendocytic itinerary of any endolyn that had reached the cell surface. Scale bar = 20 μm, (A–G); 10 μm, (H).

nonoverlapping populations of endocytic compartments en route to the apical membrane. These findings have significant implications for our understanding of how apically destined traffic may be regulated by physiological challenges.

The non-raft-associated protein endolyn traffics to the apical surface via the ARE

Rab11 localization and/or function is disrupted by overexpression of dominant-negative acting C-terminal fragments of myosin Vb and Sec15. Our findings that endolyn passes through the Rab11a-positive ARE in the biosynthetic pathway and that its appearance at the apical surface is significantly diminished upon expression of these constructs indicate that apical delivery of endolyn occurs via this compartment in a Rab11-dependent fashion. However, it is formally possible that the effects we observed upon ARE perturbation are due to inhibition of endolyn recycling rather than to a disruption in the delivery of newly synthesized protein. Unlike HA, which is very poorly internalized (Roth *et al*, 1986), endolyn is endocytosed from the apical surface at a rate of roughly

1%/min (Potter *et al*, 2006). Alternatively, it is possible that a protein required for surface delivery of endolyn-containing transport carriers is mislocalized or nonfunctional in cell lines with altered Rab11 function. Several lines of evidence argue against these alternate scenarios: first, we observed no colocalization of internalized anti-endolyn antibodies with GFP-MyoVbT, suggesting that internalized endolyn does not efficiently access the ARE, but instead recycles from apical early endosomes (AEE). Second, inactivation of HRP-WGA- or HRP-Tf-containing compartments had no effect on endolyn delivery, although these treatments would be predicted to disrupt endolyn recycling. Third, we observed kinetic effects on apical delivery of radiolabeled endolyn in MyoVbT cells after only 30 min, whereas effects on postendocytic traffic would be predicted to be mostly noticeable after longer chase periods. Finally, newly synthesized endolyn was observed to colocalize with Rab11a shortly after release from a TGN block. Thus, our data are most consistent with a functional role for the ARE in the apical delivery of newly synthesized rather than postendocytic endolyn.

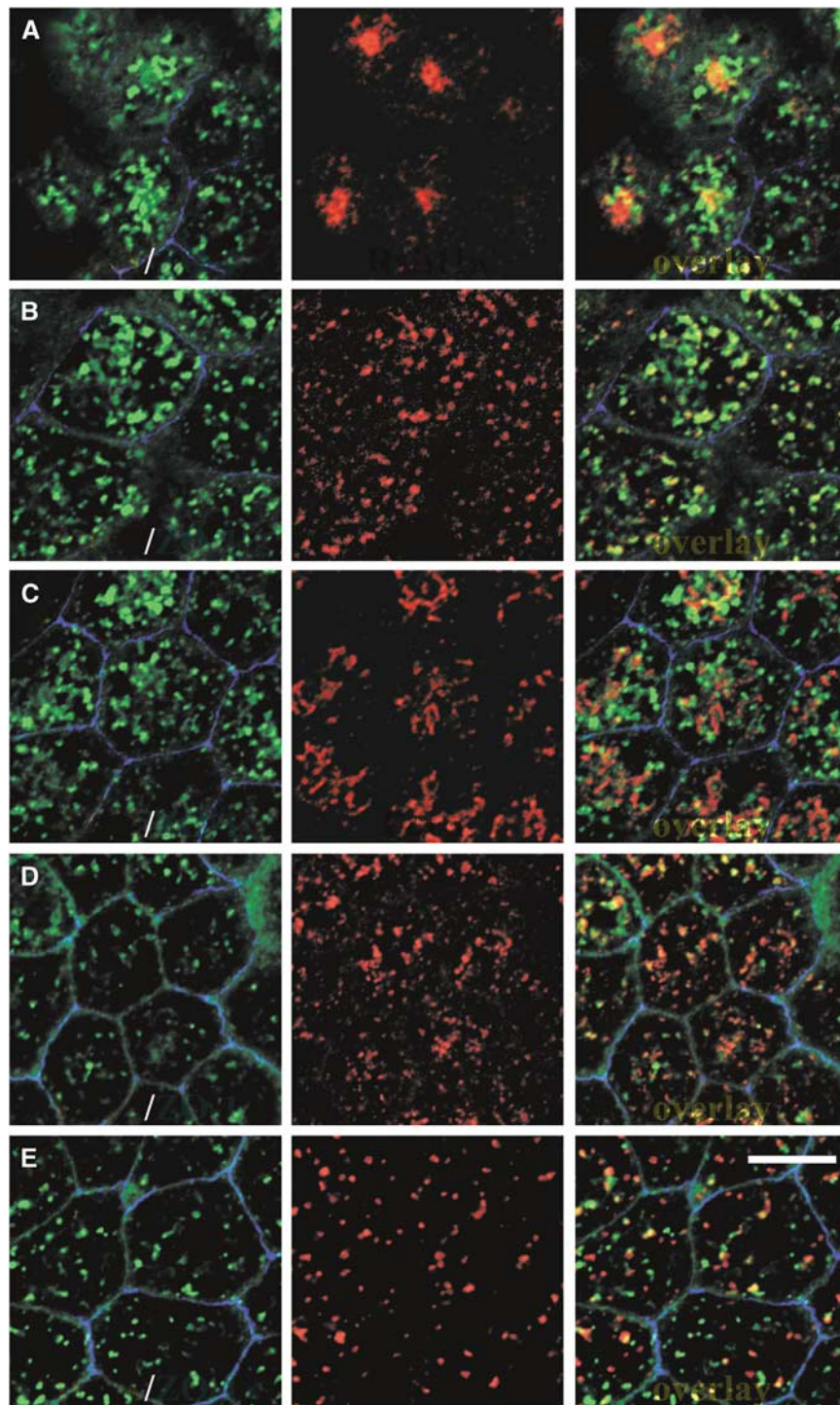


Figure 6 Characterization of WGA internalization conditions. WGA-FITC (25 $\mu\text{g}/\text{ml}$) was internalized from the apical surface of filter-grown PTR9 cells for 15 min at 37°C, and residual surface lectin was stripped with *N*-acetyl-D-glucosamine. After washing, cells were fixed, permeabilized, and processed for indirect immunofluorescence using antibodies against ZO-1 to visualize tight junctions (blue) and one of the following markers (red) (A) Rab11a, (B) EEA1, (C) furin, (D) mannose-6-phosphate receptor (M6PR), and (E) Lamp2. Single optical sections from apical-supranuclear levels of the cells are shown. Scale bar = 10 μm .

Raft-associated and raft-independent proteins take different routes to the apical membrane

Our data demonstrate striking differences in the effects of perturbing distinct endocytic compartments on the surface delivery of raft-associated versus raft-independent proteins. In contrast to endolyn, which is fully soluble in cold Triton X-100, transport of raft-associated HA was insensitive to

perturbation of Rab11 function. In contrast, delivery of HA was inhibited by inactivation of early endocytic compartments that received apically internalized HRP-WGA. Conversion of endolyn to a GPI-anchored protein resulted in efficient partitioning of this mutant into detergent-resistant membranes (DRMs) and apical delivery via a mechanism independent of *N*-glycans (Potter *et al*, 2004). Strikingly,

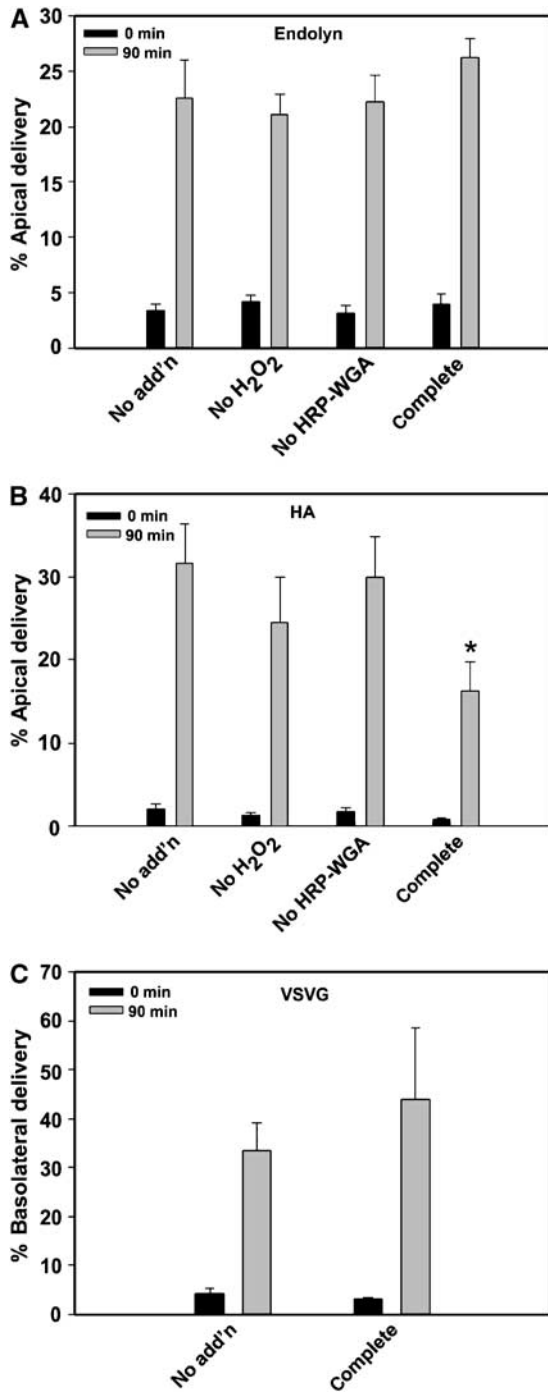


Figure 7 Inactivation of apical WGA-containing endosomes disrupts delivery of HA, but not endolyn or VSV-G. Filter-grown PTR9 or control MDCK cells infected with adenoviruses encoding endolyn (A), HA (B), or VSV-G (C) were starved for 30 min and radiolabeled for 15 min. HRP-WGA was included in the apical medium during the 15 min pulse or afterwards for 1 h at 19°C. After internalization, remaining surface HRP-WGA was removed with 100 mM *N*-acetyl-D-glucosamine before endosome inactivation as described in Materials and methods. Subsequently, cells were chased for 0 or 90 min at 37°C and apical delivery was quantified. The percent surface delivery is plotted as the mean \pm s.e.m. for endolyn ($n = 3$) and HA ($n = 6$) and as mean \pm s.d. for VSV-G ($n = 1$ experiment performed in sextuplicate). Ablation of apical WGA-containing endosomes reduced appearance of HA at the surface ($*P < 0.03$ compared with the 'no add'n' control).

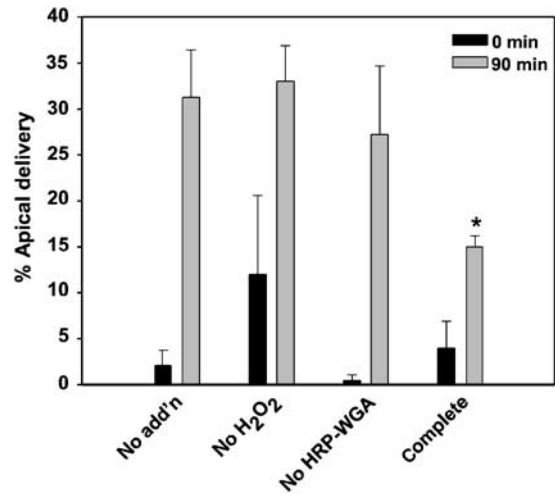


Figure 8 Inactivation of WGA-containing compartments disrupts apical delivery of GPI-linked endolyn. Filter-grown MDCK cells stably expressing GPI-anchored endolyn were incubated with 2 mM butyrate overnight at 37°C to induce protein expression. The following day, cells were radiolabeled and incubated with HRP-WGA as described in the legend to Figure 7 before quantitation of GPI-endolyn apical delivery by domain selective biotinylation. The percent surface delivery of GPI-endolyn is plotted as the mean \pm s.e.m. of three experiments. $*P < 0.05$ compared with the 'no add'n' control.

apical delivery of GPI-endolyn, like HA, was inhibited when HRP-WGA-containing compartments were ablated by DAB and H₂O₂-mediated crosslinking. Although DRMs isolated by virtue of their insolubility in cold Triton X-100 are not necessarily equivalent to the lipid rafts that exist in cells, the preference of a given protein for DRMs remains for now a fortuitous and reasonable means to distinguish lipid raft-associated and raft-independent apical markers. Indeed, as recently noted in an elegant review by Deborah Brown, there is a striking correspondence between protein association with DRMs and lipid raft-dependent functions (Brown, 2006). However, it is not yet clear whether this association is required for proper apical sorting of this class of proteins (Benting *et al*, 1999; McGwire *et al*, 1999; Paladino *et al*, 2004; Pang *et al*, 2004). For example, whereas GPI anchors have been suggested to function as apical targeting signals, the luminal domains of some GPI-anchored proteins are still secreted apically when expressed without their GPI-anchor attachment domains (Lisanti *et al*, 1989; Powell *et al*, 1991). Given our results, it would be interesting to determine whether the biosynthetic itinerary of these anchorless proteins differs from that of the native GPI protein.

Biosynthetic trafficking itinerary of raft-associated proteins

We followed two different protocols of HRP-WGA internalization (15 min at 37°C or 1 h at 19°C) to ablate apical endocytic compartments accessible to this marker. Under both conditions, WGA was detected in several intracellular compartments, including EEA1-positive AEEs, MPR-positive late endosomes, and LAMP2-positive lysosomes. However, apically internalized WGA was notably excluded from the TGN as well as from Rab11a- and Rab11b-positive apical recycling compartments. At present, we do not know which compartment(s) are functionally relevant for delivery of raft-associated proteins. DAB- and H₂O₂-mediated crosslinking after

apical incubation with 10 mg/ml HRP, a fluid phase marker that is efficiently internalized into AEE, did not disrupt apical delivery of HA, suggesting that this compartment is not accessed along the biosynthetic pathway (KO Cresawn and BA Potter, unpublished data, 2006). Because we observed that the surface stripping protocol we used for our immunofluorescence and biochemical studies sometimes left patches of residual apical FITC-WGA, we also investigated the possibility that inhibition of HA surface delivery reflected cross-linking of apical membrane components. To this end, we incubated radiolabeled HA-expressing cells with HRP-WGA at 4°C for 1 h to allow surface binding (but not internalization) of the lectin then stripped as usual, and incubated the cells with DAB and H₂O₂. Importantly, subsequent surface delivery of HA was not perturbed under these conditions (BA Potter, unpublished data, 2006). Similarly, inclusion of HRP-WGA during the radiolabeling period as well as the 90 min subsequent chase had no effect on HA delivery (KO Cresawn, unpublished data, 2006), indicating that WGA-mediated clustering did not lead to selective internalization and down-regulation of a key component(s) required for targeting or fusion of transport carriers enriched in HA. Together these results suggest that raft-associated apical proteins pass through an apical endocytic compartment different from the ARE and AEE. Recent studies show that some GPI-linked proteins are internalized into specific endosomes termed GEECs (Sabharanjak *et al*, 2002; Kalia *et al*, 2006). So far, there is no evidence that biosynthetic sorting occurs in this compartment. The relationship between these compartments and that traversed by raft-associated proteins in the biosynthetic pathway remains to be explored.

What is the physiological relevance of multiple apical trafficking routes?

In all of our experiments, we observed only a partial block in membrane traffic when we perturbed the function of endocytic compartments either by crosslinking or expression of dominant-negative inhibitors, and this was true for all of the cargo proteins we tested. The effects on membrane traffic are apparently due to kinetic delays in surface delivery rather than missorting to the opposite surface domain, as VSV-G was not missorted to the apical surface upon CRE ablation and the polarity of endolyn and HA was normal when measured after long chase times (i.e., approaching steady state; data not shown). There are several possible explanations for the lack of total inhibition. First, inactivation of specific endosomes may not have been 100% efficient and biosynthetic cargo might be routed via the remaining functional elements. As a corollary, it is possible that new 'active' endosomal compartments may form over the 90 min chase period. Second, cargo proteins may also have access to more than one biosynthetic route to the surface, so that endosome inactivation affects only a fraction of cargo. Finally, cells may upregulate a compensatory pathway when the normal delivery route for a protein is unavailable. However, we found that delivery of endolyn and HA was not further compromised when HRP-WGA-containing compartments were inactivated in MyoVbT cells to generate 'doubly inactivated' cells (Supplementary Figure 4). These results suggest that individual classes of cargo are efficiently segregated from one another and do not use multiple indirect pathways to the apical surface. However, it is possible that an alternative

direct route from the TGN to the apical surface accounts for the residual surface delivery we observed.

A priori, the presence of multiple apical trafficking routes seems unnecessarily complicated. Moreover, it is unclear why post-Golgi pathways would need to intersect endocytic compartments. Conceivably, the diversity in apical trafficking pathways represents a mechanism for the cellular regulation of apical membrane function. Polarized cells may have developed multiple trafficking routes to selectively regulate the delivery of distinct functional cohorts of apical proteins in response to physiological stimuli, such as proteins involved in maintaining epithelial barrier function or required for the regulation of ion transport. The transit of newly synthesized membrane proteins through different endosomal intermediates likely provides an added level of control to regulate the delivery of different classes of proteins to the cell surface as needed. Moreover, one could speculate that some apical proteins may contain multiple sorting signals, allowing them to be rerouted to distinct pathways in response to post-translational modifications that alter their hierarchy of targeting signals. Future studies will no doubt reveal further complexities in apical trafficking routes and sorting mechanisms.

Materials and methods

HRP-mediated crosslinking

To label Tf-containing endosomal compartments for biochemical and immunofluorescence studies, nonpolarized or polarized PTR9 cells virally expressing tsVSV-G-YFP, VSV-G, endolyn, or HA were first incubated in serum-free media for 30 min to starve the cells of Tf. HRP-Tf (10 µg/ml; human, Jackson ImmunoResearch Laboratories, West Grove, PA) was internalized from the basolateral surface for 45 min at 37°C. For biochemical studies, cells were starved in media devoid of cysteine and methionine for the first 30 min of the HRP-Tf uptake and radiolabeled with 1 mCi/ml Trans-[³⁵S]-label during the last 15 min of the uptake. For cells expressing tsVSV-G-YFP, these steps were performed at 40°C rather than 37°C. HRP-Tf remaining at the cell surface was removed after two 5 min incubations with 0.5 M NaCl and 20 mM citric acid (pH 5.0). To label WGA-containing endosomal compartments, cells were incubated with apically added HRP-WGA (25 µg/ml; EY Laboratories, San Mateo, CA) during the 15 min radiolabel pulse or afterwards for 1 h at 19°C. HRP-WGA remaining at the surface was removed by three 10-min incubations with 100 mM *N*-acetyl-D-glucosamine (Sigma). To characterize the intracellular distribution of WGA under these internalization conditions, WGA-FITC (25 µg/ml) was internalized as above, the cell surface was stripped, and filters were processed for immunofluorescence.

For HRP inactivation, cells were first washed for 3 × 5 min in PBS and then incubated with PBS containing 0.1 mg/ml DAB (Sigma) and 0.025% H₂O₂. Cells were incubated in the dark on ice for 1 h. The reaction was quenched in PBS containing 1% BSA (Sigma) for 5 min and then washed three times with PBS. As controls, HRP-Tf or HRP-WGA was not internalized and samples were not incubated with DAB and H₂O₂ (no add'n), whereas in other samples only the H₂O₂ or HRP-Tf/HRP-WGA was omitted (no H₂O₂ or no HRP-Tf/no HRP-WGA, respectively). For immunofluorescence studies, non-polarized PTR9 cells expressing tsVSV-G-YFP were chased in the presence of cycloheximide at 32°C for 1 h. For biochemical studies, PTR9 cells expressing tsVSV-G-YFP were chased for 0 or 90 min at 32°C and PTR9 cells expressing VSV-G, endolyn or HA were chased at 37°C for 0 or 90 min. At each time point, delivery to the surface was quantitated. For cells expressing VSV-G or endolyn, domain-selective biotinylation of the basolateral or apical surface was performed as described previously (Altschuler *et al*, 2000). After biotinylation, cells were solubilized and immunoprecipitated with antibodies against endolyn or VSV-G and collected using fixed *Staphylococcus aureus* (CalBiochem, San Diego, CA). After elution of antibody-antigen complexes, one-fifth of the immunoprecipi-

tated sample was reserved to calculate the total amount of radioactive cargo and the remainder was incubated with streptavidin agarose to recover the biotinylated fraction. Samples were quantitated after SDS-PAGE using a phosphorimager. The % delivery of each cargo was calculated as the amount biotinylated relative to the total recovered at each time point. Apical delivery of HA was quantitated by cell surface trypsinization as described by Henkel *et al* (2000). Cleavage of cell surface HA by low concentrations of TPCK-treated trypsin (20 µg/ml) generates two fragments that remain covalently associated via disulfide bonds and which co-isolate upon immunoprecipitation with our monoclonal antibody. Upon electrophoresis under reducing conditions, the two fragments (marked HA1 and HA2 in Figure 2) are clearly resolved from one another as well as from uncleaved (intracellular) HA (HA0). Although the efficiencies of surface biotinylation and trypsinization varied between experiments, we consistently found the same trends with respect to the effect of a given perturbant (HRP-ligand or dominant-negative mutant) regardless of the overall efficiency of transport. Statistical significance was assessed using Student's *t*-test unless otherwise indicated.

IgA uptake

Filter-grown control MDCK cells or cells expressing GFP-tagged MyoVbT cells were rinsed three times with warm MEM-BSA (modified Eagle's medium with Hank's balanced salts, 0.6% (w/v) BSA, and 20 mM Hepes, pH 7.4) and incubated basolaterally with

200 µg/ml of dimeric human IgA (purchased from Dr JP Vaerman, Catholic University of Louvain, Belgium) for 10 min at 37°C. The cells were rinsed five times over a 1-h period at 37°C with MEM-BSA, then fixed and processed to detect GFP-MyoVbT and endolyn.

Cell lines, antibodies, adenoviruses, and immunofluorescence are described in the Supplementary data.

Supplementary data

Supplementary data are available at *The EMBO Journal* Online (<http://www.embojournal.org>).

Acknowledgements

We thank Douglas Lyles, Thomas Braciale, Enrique Rodriguez-Boulant, Silvia Corvera, Linton Traub, Daniel Goodenough, Patrick Keller, and Michael Roth for gifts of antibodies, viruses, and cell-lines. We are grateful to Nancy Zurowski and the Ophthalmology FACS Lab at the University of Pittsburgh and the Core Grant for Vision Research (EY08098) for assistance with cell sorting. This work was supported in part by NIDDK National Institutes of Health grants DK54407 (to O.A.W.) and DK54425 and DK51970 (to G.A.). KO Cresawn was supported by a postdoctoral fellowship from the American Heart Association, and BA Potter, AO, and CJG were supported by American Heart Association predoctoral fellowships.

References

- Altschuler Y, Kinlough CL, Poland PA, Bruns JB, Apodaca G, Weisz OA, Hughey RP (2000) Clathrin-mediated endocytosis of MUC1 is modulated by its glycosylation state. *Mol Biol Cell* **11**: 819–831
- Ang AL, Taguchi T, Francis S, Folsch H, Murrells LJ, Pypaert M, Warren G, Mellman I (2004) Recycling endosomes can serve as intermediates during transport from the Golgi to the plasma membrane of MDCK cells. *J Cell Biol* **167**: 531–543
- Apodaca G, Katz LA, Mostov KE (1994) Receptor-mediated transcytosis of IgA in MDCK cells is via apical recycling endosomes. *J Cell Biol* **125**: 67–86
- Barroso M, Sztul ES (1994) Basolateral to apical transcytosis in polarized cells is indirect and involves BFA and trimeric G protein sensitive passage through the apical endosome. *J Cell Biol* **124**: 83–100
- Benting JH, Rietveld AG, Simons K (1999) N-Glycans mediate the apical sorting of a GPI-anchored, raft-associated protein in Madin–Darby canine kidney cells. *J Cell Biol* **146**: 313–320
- Brown DA (2006) Lipid rafts, detergent-resistant membranes, and raft targeting signals. *Physiology (Bethesda)* **21**: 430–439
- Brown PS, Wang E, Aroeti B, Chapin SJ, Mostov KE, Dunn KW (2000) Definition of distinct compartments in polarized Madin–Darby canine kidney (MDCK) cells for membrane-volume sorting, polarized sorting and apical recycling. *Traffic* **1**: 124–140
- Ellis MA, Potter BA, Cresawn KO, Weisz OA (2006) Polarized biosynthetic traffic in renal epithelial cells: sorting, sorting, everywhere. *Am J Physiol Renal Physiol* **291**: F707–F713
- Futter CE, Connolly CN, Cutler DF, Hopkins CR (1995) Newly synthesized transferrin receptors can be detected in the endosome before they appear on the cell surface. *J Biol Chem* **270**: 10999–11003
- Gibson A, Futter CE, Maxwell S, Allchin EH, Shipman M, Kraehenbuhl JP, Domingo D, Odorizzi G, Trowbridge IS, Hopkins CR (1998) Sorting mechanisms regulating membrane protein traffic in the apical transcytotic pathway of polarized MDCK cells. *J Cell Biol* **143**: 81–94
- Guerrero CJ, Weixel KM, Bruns JR, Weisz OA (2006) Phosphatidylinositol 5-kinase stimulates apical biosynthetic delivery via an Arp2/3-dependent mechanism. *J Biol Chem* **281**: 15376–15384
- Heine M, Cramm-Behrens CI, Ansari A, Chu HP, Ryazanov AG, Naim HY, Jacob R (2005) Alpha-kinase 1, a new component in apical protein transport. *J Biol Chem* **280**: 25637–25643
- Henkel JR, Gibson GA, Poland PA, Ellis MA, Hughey RP, Weisz OA (2000) Influenza M2 proton channel activity selectively inhibits *trans*-Golgi network release of apical membrane and secreted proteins in polarized Madin–Darby canine kidney cells. *J Cell Biol* **148**: 495–504
- Hoekstra D, Tyteca D, van IJendoorn SC (2004) The subapical compartment: a traffic center in membrane polarity development. *J Cell Sci* **117**: 2183–2192
- Ihrke G, Bruns JR, Luzio JP, Weisz OA (2001) Competing sorting signals guide endolyn along a novel route to lysosomes in MDCK cells. *EMBO J* **20**: 6256–6264
- Ihrke G, Kytala A, Russell MR, Rous BA, Luzio JP (2004) Differential use of two AP-3-mediated pathways by lysosomal membrane proteins. *Traffic* **5**: 946–962
- Jacob R, Heine M, Alfalah M, Naim HY (2003) Distinct cytoskeletal tracks direct individual vesicle populations to the apical membrane of epithelial cells. *Curr Biol* **13**: 607–612
- Jacob R, Naim HY (2001) Apical membrane proteins are transported in distinct vesicular carriers. *Curr Biol* **11**: 1444–1450
- Kalia M, Kumari S, Chadda R, Hill MM, Parton RG, Mayor S (2006) Arf6-independent GPI-anchored protein-enriched early endosomal compartments fuse with sorting endosomes via a Rab5/ phosphatidylinositol-3'-kinase-dependent machinery. *Mol Biol Cell* **17**: 3689–3704
- Keller P, Toomre D, Diaz E, White J, Simons K (2001) Multicolour imaging of post-Golgi sorting and trafficking in live cells. *Nat Cell Biol* **3**: 140–149
- Kreitzer G, Schmoranzler J, Low SH, Li X, Gan Y, Weimbs T, Simon SM, Rodriguez-Boulant E (2003) Three-dimensional analysis of post-Golgi carrier exocytosis in epithelial cells. *Nat Cell Biol* **5**: 126–136
- Lapierre LA, Kumar R, Hales CM, Navarre J, Bhartur SG, Burnette JO, Provance Jr DW, Mercer JA, Bahler M, Goldenring JR (2001) Myosin vb is associated with plasma membrane recycling systems. *Mol Biol Cell* **12**: 1843–1857
- Leitinger B, Hille-Rehfeld A, Spiess M (1995) Biosynthetic transport of the asialoglycoprotein receptor H1 to the cell surface occurs via endosomes. *Proc Natl Acad Sci USA* **92**: 10109–10113
- Lin S, Naim HY, Rodriguez AC, Roth MG (1998) Mutations in the middle of the transmembrane domain reverse the polarity of transport of the influenza virus hemagglutinin in MDCK epithelial cells. *J Cell Biol* **142**: 51–57
- Lisanti MP, Caras IW, Davitz MA, Rodriguez-Boulant E (1989) A glycopospholipid membrane anchor acts as an apical targeting signal in polarized epithelial cells. *J Cell Biol* **109**: 2145–2156

- Lock JG, Stow JL (2005) Rab11 in recycling endosomes regulates the sorting and basolateral transport of E-cadherin. *Mol Biol Cell* **16**: 1744–1755
- McGwire GB, Becker RP, Skidgel RA (1999) Carboxypeptidase M, a glycosylphosphatidylinositol-anchored protein, is localized on both the apical and basolateral domains of polarized Madin–Darby canine kidney cells. *J Biol Chem* **274**: 31632–31640
- Orzech E, Cohen S, Weiss A, Aroeti B (2000) Interactions between the exocytic and endocytic pathways in polarized Madin–Darby canine kidney cells. *J Biol Chem* **275**: 15207–15219
- Oztan A, Silvis M, Weisz OA, Bradbury NA, Hsu S-C, Goldenring JR, Yeaman C, Apodaca G (in press) Exocyst requirement for endocytic traffic directed toward the apical and basolateral poles of polarized MDCK cells. *Mol Biol Cell*
- Paladino S, Sarnataro D, Pillich R, Tivodar S, Nitsch L, Zurzolo C (2004) Protein oligomerization modulates raft partitioning and apical sorting of GPI-anchored proteins. *J Cell Biol* **167**: 699–709
- Pang S, Urquhart P, Hooper NM (2004) N-glycans, not the GPI anchor, mediate the apical targeting of a naturally glycosylated, GPI-anchored protein in polarised epithelial cells. *J Cell Sci* **117**: 5079–5086
- Polishchuk R, Di Pentima A, Lippincott-Schwartz J (2004) Delivery of raft-associated, GPI-anchored proteins to the apical surface of polarized MDCK cells by a transcytotic pathway. *Nat Cell Biol* **6**: 297–307
- Potter BA, Ihrke G, Bruns JR, Weixel KM, Weisz OA (2004) Specific N-glycans direct apical delivery of transmembrane, but not soluble or glycosylphosphatidylinositol-anchored forms of endolyn in Madin–Darby canine kidney cells. *Mol Biol Cell* **15**: 1407–1416
- Potter BA, Weixel KM, Bruns JR, Ihrke G, Weisz OA (2006) N-glycans mediate apical recycling of the sialomucin endolyn in polarized MDCK cells. *Traffic* **7**: 146–154
- Powell SK, Lisanti MP, Rodriguez-Boulan EJ (1991) Thy-1 expresses two signals for apical localization in epithelial cells. *Am J Physiol* **260**: C715–C720
- Rodriguez-Boulan E, Kreitzer G, Musch A (2005) Organization of vesicular trafficking in epithelia. *Nat Rev Mol Cell Biol* **6**: 233–247
- Roth MG, Doyle C, Sambrook J, Gething MJ (1986) Heterologous transmembrane and cytoplasmic domains direct functional chimeric influenza virus hemagglutinins into the endocytic pathway. *J Cell Biol* **102**: 1271–1283
- Sabharanjak S, Sharma P, Parton RG, Mayor S (2002) GPI-anchored proteins are delivered to recycling endosomes via a distinct cdc42-regulated, clathrin-independent pinocytic pathway. *Dev Cell* **2**: 411–423
- Wandinger-Ness A, Bennett MK, Antony C, Simons K (1990) Distinct transport vesicles mediate the delivery of plasma membrane proteins to the apical and basolateral domains of MDCK cells. *J Cell Biol* **111**: 987–1000
- Wu S, Mehta SQ, Pichaud F, Bellen HJ, Quijcho FA (2005) Sec15 interacts with Rab11 via a novel domain and affects Rab11 localization *in vivo*. *Nat Struct Mol Biol* **12**: 879–885
- Yeaman C, Le Gall AH, Baldwin AN, Monlauzeur L, Le Bivic A, Rodriguez-Boulan E (1997) The O-glycosylated stalk domain is required for apical sorting of neurotrophin receptors in polarized MDCK cells. *J Cell Biol* **139**: 929–940
- Zhang XM, Ellis S, Sriratana A, Mitchell CA, Rowe T (2004) Sec15 is an effector for the Rab11 GTPase in mammalian cells. *J Biol Chem* **279**: 43027–43034